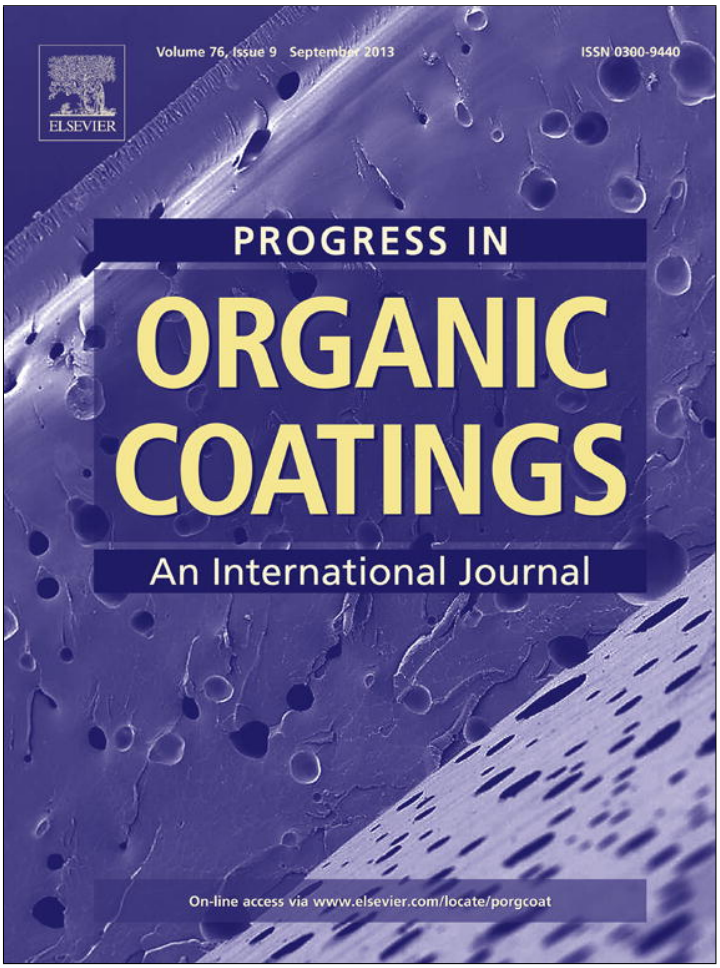

Progress in Organic Coatings 76 (2013) 1178–1183

Contents lists available at SciVerse ScienceDirect

Progress in Organic Coatings

journal homepage: www.elsevier.com/locate/porgcoat

Hydrophobic benzoxazine-cured epoxy coatings for corrosion protection

Changlu Zhou[a], Xin Lu[a], Zhong Xin[a,*], Juan Liu[a], Yanfeng Zhang[b]

[a] State Key Laboratory of Chemistry Engineering, School of Chemical Engineering, East China University of Science and Technology, Shanghai 200237, China
[b] Lanpec Technologies Co., Ltd, Gansu 730070, China

ARTICLE INFO

Article history:
Received 10 December 2012
Received in revised form 19 March 2013
Accepted 26 March 2013
Available online 18 April 2013

Keywords:
Corrosion protection
Benzoxazine
Epoxy
Curing agent
Hydrophobicity

ABSTRACT

A hydrophobic benzoxazine-cured epoxy coating (EPB) was prepared by a dip coating and thermal curing method using benzoxazine monomer (B-TMOS) as curing agent. Fourier transform infrared (FTIR) analyses confirmed the presence of thermal curing reactions and hydrogen-bonding interactions in the epoxy/polybenzoxazine system. The hydrophobicity of epoxy coatings induced by the incorporation of B-TMOS was enhanced significantly, and the water contact angles of resultant EPB coatings were higher than 98°. The corrosion protection ability of epoxy coatings was investigated by open-circuit potentials, potentiodynamic polarization curves and electrochemical impedance spectroscopy (EIS) methods. The results showed that the charge transfer resistance (R_{ct}) of EPB coatings was increased by about three orders of magnitude compared with bare mild steel, and the protection efficiency values of all EPB samples were more than 98%. This increased corrosion protection property could be attributed to the high hydrophobic performance of EPB coatings.

1. Introduction

Metallic corrosion causes considerable waste of natural resources. The annual cost of corrosion worldwide is estimated to exceed US$ 1.8 trillion, which translates to 3–4% of the gross domestic product (GDP) of industrialized countries, even surpassing the loss caused by natural hazards [1]. Organic coatings have been employed to protect steel surfaces against versatile corrosion environments for a long time by introducing a barrier to prevent ionic transport and electrical conduction. The hydrophobic properties, water uptake and cross-linking density of the coating influence its ability for isolating the steel from corrosive electrolyte [2–6].

In the past decade, epoxy resins have been widely used as a coating material for corrosion protection, owing to its outstanding processability, excellent chemical resistance, high cross-linking density, and strong adhesion/affinity to substrates [7,8]. However, the high water uptake and hydrophilic nature of epoxy resins have hindered its application in humid conditions. Not only the absorbed water can deteriorate the thermal and mechanical properties of resin, but can also initiate corrosion reactions on the metallic substrates [9–11]. Hence, a lot of efforts have been made to improve the water resistance of epoxy coatings. Guo et al. [12] investigated nanostructured thermosets containing epoxy and poly(ε-caprolactone)-block-poly(dimethyl siloxane)-block-poly(ε-caprolactone) (PCL-PDMS-PCL) triblock copolymers. This study showed that the water contact angle (CA) of ER/PCL–PDMS–PCL blends increased significantly with higher triblock copolymer concentrations, with CA > 80° at 60 wt% PCL–PDMS–PCL. Sordo et al. [13] incorporated PDMS additives into epoxy resins by a physical method, improving the surface properties of the cured materials without affecting the good adhesion properties of the epoxy films on polar substrates. Cui et al. [14] also reported that the synthesis of semi-interpenetrating fluorine-containing polyacrylate and epoxy resin with different fluorine content could improve the hydrophobic property of polymer networks. However, phase separation might occur due to the incompatibility of the incorporated additive along with the curing agent in these studies. Moreover, although fluoropolymers are favorable compounds for modifying the surface properties of coatings, the relatively high market price of such materials limit their applications. Therefore, it is of great interest to develop a kind of economic material to modify surface properties of epoxy coatings, which also has good compatibility with epoxy resins.

Recently, significant progress has been achieved on the cocrosslinking of benzoxazine with epoxy, whereby benzoxazine is used as a curing agent of epoxy due to the reaction between the phenolic —OH groups of the ring-opened benzoxazine and epoxide groups. It is believed that incorporation of polybenzoxazine into the epoxy network structure will result in excellent heat resistance, flame resistance, electrical insulation and mechanical performance [15–20]. Furthermore, polybenzoxazine is a class of thermoset resins with low surface energy, far lower than that of pure Teflon® [21,22]. In addition, non-fluorinated polybenzoxazine could remarkably reduce the production cost [23,24]. Above all, the

* Corresponding author. Tel.: +86 21 64240862; fax: +86 21 64251772.
E-mail address: xzh@ecust.edu.cn (Z. Xin).

0300-9440/$ – see front matter © 2013 Elsevier B.V. All rights reserved.
http://dx.doi.org/10.1016/j.porgcoat.2013.03.013

hydrophobic properties of epoxy coatings can be improved by utilizing benzoxazine as a curing agent, and this benzoxazine-cured epoxy may have the potential to be applied as a low-cost hydrophobic coating material for corrosion protection.

The focus of the present work is to apply a polybenzoxazine precursor (B-TMOS) as epoxy curing agent. The B-TMOS cured epoxy (EPB) coatings were prepared by dip coating and thermal curing method. Fourier transform infrared (FTIR) spectroscopy was used to characterize the structure of the coatings. In particular, the changes in the surface properties of hydrophilic epoxy coatings upon the addition of hydrophobic B-TMOS were examined by contact angle measurement. Finally, the potential of EPB as a corrosion protective coating for Q235B mild steel (MS) electrodes is investigated by electrochemical measurements.

2. Experimental

2.1. Materials and reagents

The mild steel (MS) (Q235B, composition in wt%: C: 0.12, Mn: 0.32, Cr: 0.035, Si: 0.14, Ni: 0.040, S: 0.010, P: 0.012, Cu: 0.010, Fe: balance) was provided by Lanpec Technologies Co. Ltd, China. Bisphenol A and 4, 4′-diaminodiphenyl methane (DDM) were purchased from Sinopharm Chemical Reagent Co. Ltd, China. 3-Aminopropyltrimethoxysilane (3-APTMOS) was obtained from Diamond Advanced Material of Chemical Inc., China. Epoxy resins (type E-51, 0.53 eq/100 g) were purchased from Shanghai Resin Factory Co., Ltd, China. Paraformaldehyde, chloroform, xylene, n-butanol and other chemicals were from Shanghai Lingfeng Chemical Corp., China. All chemicals were of analytical pure reagent grade. Chloroform was purified by distillation over calcium hydride (CaH_2) prior to use; all other chemicals were used as received.

2.2. Synthesis of benzoxazine monomer

2,2-Bis (3-(trimethoxysilyl)-n-propyl-3,4-dihydro-2H-1, 3-benzoxazine)propane (B-TMOS) was synthesized by a method available in the literature (Scheme 1) [22,25]. The product was yellow liquid with a yield of 85.1%. FTIR (KBr): ν = 1498 (tri-substituted phenyl group); 1231 (s; ν_{as} (C—O—C of benzoxazine ring)), 1016 (s; ν_s (C—O—C of benzoxazine ring)); 1085 (s; ν_{as} (Si—O—C)); 931 (oxazine ring). ^{1}H NMR (400 MHz, chloroform-d, δ): 6.75–7.26 (m, 6H, ArH), 4.82 (s, 4H, O—CH_2—N), 3.98 (s, 4H, Ph—CH_2—N), 3.58 (s, 18H, Si—O—CH_3), 2.73 (t, 4H, N—CH_2), 1.66 (m, 4H, —CH_2—CH_2Si), 0.67 (t, 4H, —CH_2—Si).

2.3. Sample preparation and coating method

Bare MS was used as substrate. The substrates were blasted to Sa 2 1/2 and then degreased with acetone. DDM-cured epoxy (EPD) was prepared by reacting of 30 wt% DDM with E-51. B-TMOS-cured epoxy (EPB) was prepared by reacting of different ratios of B-TMOS mixed with E-51. The structure of E-51 is shown in Scheme 2. MS plates were dip coated into the epoxy solution for uninterrupted six times with a withdraw speed of 320 mm min^{-1}. The substrates remained in the solution for 1 min every time. The EPD sample was polymerized at 80 and 150 °C, each for 2 h, respectively. The EPB samples were cured in one step at 230 °C for 2 h. Samples obtained by reacting 10 wt%, 20 wt%, 30 wt% and 40 wt% B-TMOS with E-51 were labeled EPB10, EPB20, EPB30 and EPB40, respectively. The thickness of the coatings was evaluated on the stainless steel surfaces before and after coating using a micrometer (Mitutoyo, Japan), resulting on thicknesses of ~5 μm for all coatings.

2.4. Characterization

2.4.1. Fourier transforms infrared (FTIR) spectroscopy

FTIR measurements were carried out on a Nicolet iS10 FTIR spectrometer at room temperature (~25 °C) using the KBr pellet method. In all cases, 32 scans at a resolution of 1 cm^{-1} were recorded. The samples were prepared by casting the mixture solution onto a KBr plate, and then the residual solvent was removed by drying in vacuum. Some of the samples were further cured at a given condition to form polymer films.

2.4.2. Surface properties

Static contact angles of the samples were determined by contact angle goniometry at 25 °C using a DataPhysicsOCA20 optical goniometer interfaced with image-capture software by injecting a 2 μL liquid drop. Deionized water was used as the test liquid. In order to obtain reliable contact angle data, five droplets were dispensed at different regions of the films.

2.4.3. Adhesion measurement

A knife was used to make a cross-cut pattern (space the cuts 1 mm apart and make 11 cuts) at 90° angles throughout the coating. The coating was brushed lightly with a soft brush after each cut to remove debris from the surface. Scotch 600 tape was applied to the cut surface and rubbed with the eraser end of a pencil to ensure good attachment to the coating, and then the tape was removed after 90 s [4,26].

2.5. Corrosion evaluations

Electrochemical measurements were measured with a CH Instruments CHI660D (USA) workstation with a three-electrode system. The coated sample acted as the working electrode, a Ag/AgCl (saturated KCl) electrode was used as the reference electrode, and a stainless steel cylinder as the counter electrode. The electrodes working area was ~14 cm^2. Electrochemical corrosion measurements were investigated using a potentiodynamic polarization technique, open circuit potential (E_{ocp})–time curves and electrochemical impedance spectroscopy (EIS). All tests were performed in a corrosive medium (3.5 wt% NaCl aqueous solution) at ambient temperature. Samples were immersed for 30 min to ensure the steady-state prior to measurements; measurements were repeated at least three times. In the polarization current experiments, the potential was scanned from −100 mV below to +100 mV vs Ag/AgCl above the corrosion potential E_{corr} at a scan rate of 2 mV s^{-1}. The corrosion current I_{corr} and E_{corr} were obtained automatically from the Tafel plots using the CHI660D workstation analysis software. In the electrochemical impedance spectroscopy (EIS) measurements, a sinusoidal AC perturbation of 10 mV amplitude coupled with the open circuit potential was applied to the metal/coating system. The EIS test was managed in the frequency range from 100 kHz to 0.01 Hz. EIS analysis was performed by using Zview software.

3. Results and discussion

3.1. Structure characterization of EPB

In order to determine that both epoxy precursive and B-TMOS monomeric species were participating in the curing reaction, a qualitative infra-red analysis was undertaken for cured samples with different B-TMOS content compared with E-51 precursor and B-TMOS monomer, shown in Fig. 1. The benzoxazine ring is characterized by the absorption peak at 931 cm^{-1}, corresponding to out plane bending vibrations of C—H of the oxazine ring [22,27]. The disappearance of the oxazine band indicated that oxazine rings

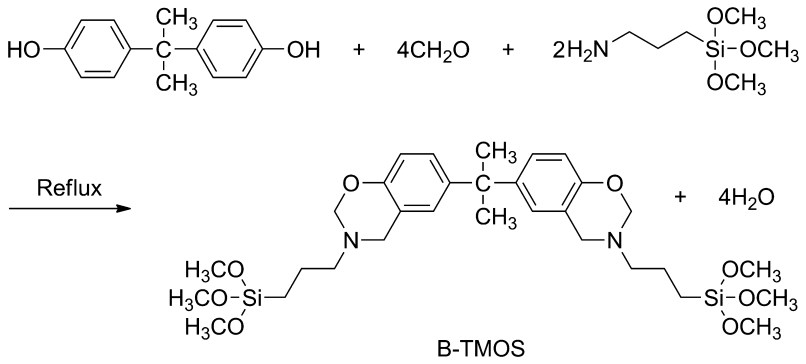

Scheme 1. Synthesis route of benzoxazine monomer (B-TMOS).

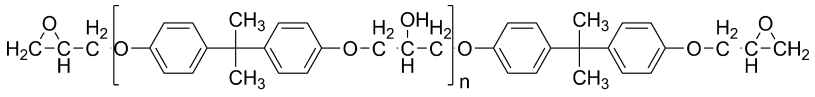

Scheme 2. The chemical structure of E-51.

in all EPB samples were opened completely and participated in the polymerization reaction after curing at 230 °C for 2 h. Since polybenzoxazine acted as an epoxy polymerization initiator and catalyst in the curing reaction [16,17], epoxy polymerization took place concurrently with the benzoxazine polymerization. The consumption of epoxy could be monitored by the disappearance of the 916 cm^{-1} and 863 cm^{-1} epoxide ring modes as the ring was opened [18]. As seen in Fig. 1, the epoxide peaks almost disappeared in all EPB samples. Thus, as showed in Scheme 3 there would be polybenzoxazine network formed by the oxazine ring opening reaction (part A in Scheme 3) linked with epoxy network by the etherification hydroxyl-oxazine reaction (part B in Scheme 3) for all EPB samples.

The hydroxyl stretching region (4000–2500 cm^{-1}) in the infrared spectra of EPB samples is shown in Fig. 2. Generally, epoxy is a self-associating polymer because of the presence of hydroxyl groups [12]. EPB10 showed a distinct band in the hydroxyl region. A broad band centered at 3447 cm^{-1} was observed in Fig. 2, which could be mainly attributed to the stretching vibrations of self-associated hydroxyl groups (part D in Scheme 3). Also, the band at 3447 cm^{-1} shifted to lower frequencies with the increase in the B-TMOS content. This verified the formation of —OH···O intermolecular hydrogen bonding between the hydroxyl groups of the epoxy and phenolic hydroxyl groups of poly(B-TMOS) (part C in Scheme 3). Furthermore, a shoulder band at 3626 cm^{-1} corresponding to nonassociative free hydroxyl groups was detected when the B-MTOS content was more than 30 wt%. It is suggested that the excess phenolic hydroxyl groups of benzoxazine formed hydrogen bonding with epoxy when the content of B-TMOS was high enough (>30 wt%). Hence, the —OH groups generated by the oxazine ring opening reaction should not only react with the epoxide groups of epoxy, but also participated in the formation of

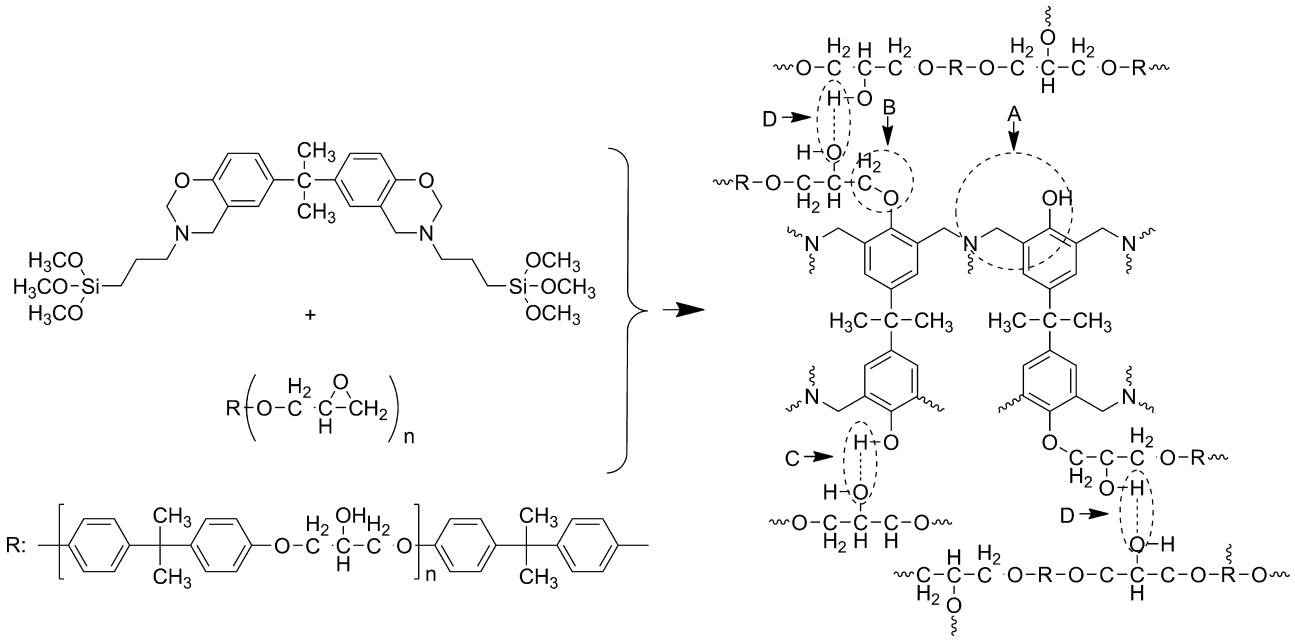

Scheme 3. Schematic diagram illustrating the process of copolymerization ((A) thermal induced oxazine ring opening; (B) etherification hydroxyl-oxazine reaction; (C) hydrogen bonding interaction between polybenzoxazine and epoxy: self-associated hydroxyl groups of epoxy).

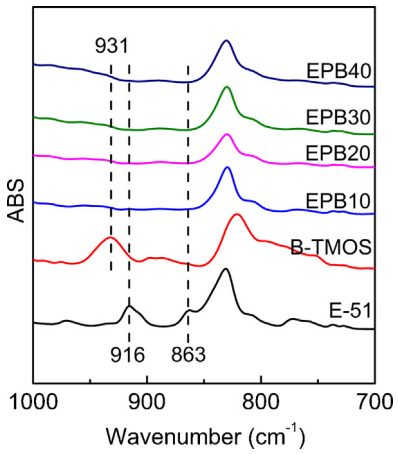

Fig. 1. FTIR spectra over the region of 1000–700 cm^{-1} for E-51, B-TMOS monomer and EPB samples.

intermolecular hydrogen bonding with hydroxyl groups of epoxy. The fraction of intermolecular hydrogen bonding between epoxy and poly(B-TMOS) increased with increasing B-TMOS content according to the FTIR spectra analyses (Fig. 2).

In summary, the phenolic —OH groups generated by the oxazine ring opening reaction reacted with the epoxide ring to initiate the epoxy polymerization, and participated in the intermolecular hydrogen-bonding interaction between them simultaneously. The compatibility of epoxy/PB-TMOS blend system could be enhanced by the hydrogen bonding interactions.

3.2. Surface properties of EPB coatings

Epoxy coatings with different ratios of B-TMOS at 10%, 20%, 30% and 40% by weight were prepared through a dip coating and thermal curing method. It was found that the benzoxazine concentration had a crucial effect on film formation. In previous studies, only copolymers with more than 57 wt% benzoxazine were successfully cured for phenyl based benzoxazine/epoxy copolymers. Samples with low benzoxazine content were still in liquid state after curing [18]. But in our system, even samples with a low content of 20 wt% B-TMOS formed uniform, smooth and optically transparent films, which showed that silane-functional benzoxazine had better compatibility with epoxy than phenyl based benzoxazine. All EPB samples were homogenous and transparent at room temperature when the content of B-TMOS was more than 20 wt%. However, there were obvious defects in EPB10 samples, which were excluded from the contact angle measurements and corrosion resistance analysis. These defects results from

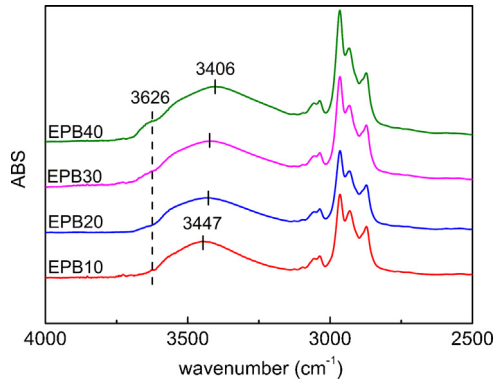

Fig. 2. FTIR spectra over the region of 4000–2500 cm^{-1} for EPB samples.

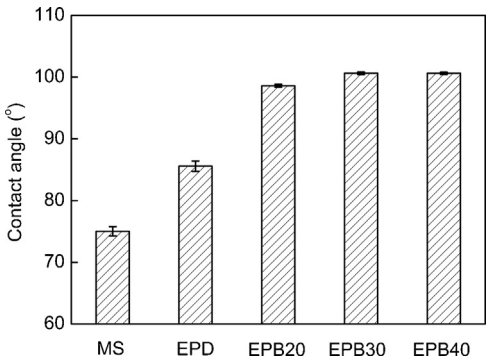

Fig. 3. Variation of the water contact angle on the surfaces of bare MS and epoxy coatings with different curing agents.

incomplete cure were due to the fact that insufficient catalyst (B-TMOS) for curing the epoxy was added to the blend system.

Contact angle measurements were taken for bare MS, EPD and EPB coated samples in order to investigate the surface hydrophobicity, shown in Fig. 3. Generally speaking, larger contact angles imply more hydrophobic surfaces[28,29]. The contact angle of the DDM cured epoxy coating was 85.5 ± 0.9°, only 10° higher than for bare MS at 75.0 ± 0.7°; meanwhile for EPB samples were 98.6 ± 0.3° for EPB20 and more than 100° for EPB30 and EPB40. The hydrophobicity of epoxy coatings was significantly improved even at low B-TMOS content. This increased hydrophobicity might decrease the wettability of aggressive electrolytes, which could be limited on the PB-TMOS coating surface. The barrier for corrosion under prolonged contact with aggressive media would be improved due to very low portion of coating area was in real contact with electrolyte solution [30–32]. Additionally, the adhesion of all samples was investigated by the cross-cut method. There was no significant detachment of either EPB or EPD after cross-cutting, and all the edges of the cuts were smooth. It is evident that adhesion between MS and both coatings was strong. In other words, the hydrophobicity of epoxy was improved by incorporating B-TMOS without loss of its adhesion. This is likely caused because the alkoxy groups of B-TMOS could be hydrolyzed in the moist environment during the dip coating process and convert to silanols (SiOH), which could easily react with hydroxyl groups on the metal surface and convert to Fe—O—Si bonds at the interface between substrate and EPB coating [23,29,33].

3.3. Corrosion resistance of EPB coatings

The corrosion resistance of the prepared coatings in 3.5 wt% NaCl aqueous solution was evaluated by the open-circuit potentials (E_{ocp}), potentiodynamic polarization curves and EIS approaches. The E_{ocp} recorded for bare and coated MS were plotted as a function of immersion time shown in Fig. 4. Initial E_{ocp} value of uncoated MS and EPD coated MS were −0.687 V vs Ag/AgCl and −0.478 V vs Ag/AgCl, which decreased to −0.731 V and −0.567 V vs Ag/AgCl after 90 min of immersion time, respectively. However, initial E_{ocp} values of EPB20, EPB30, EPB40 electrodes were −0.482, −0.468 and −0.456 V vs Ag/AgCl, respectively, which were more positive compare to uncoated MS and EPD samples even after 90 min exposure to 3.5 wt% NaCl aqueous solution. According to Fig. 4, the E_{ocp} was shifted to the noble values when B-TMOS monomer was used as a curing agent for epoxy coating. High E_{ocp} values typically indicate high corrosion resistance of coatings [34]. The increased E_{ocp} suggests that EPB coatings are less porous with a lower permeability against diffusing corrosive species [35,36], significantly enhancing the barrier properties when using B-TMOS as curing agent. The number of free volumes inside the coating matrix might

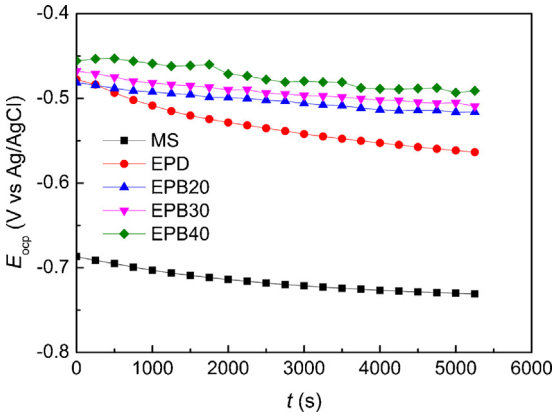

Fig. 4. The E_{ocp}–time curves for different electrodes in 3.5 wt% NaCl aqueous solutions.

significantly decrease due to the dual cross-linking and hydrogen-bonding network of polybenzoxazine and epoxy.

Fig. 5 shows the Tafel curves of bare and coated MS in 3.5 wt% NaCl solutions. The corrosion potential E_{corr} and corrosion current density I_{corr} of different samples could be obtained by the Tafel extrapolation method [5]. The corrosion rate (CR) was calculated using the I_{corr} values and Eq. (1) [37]:

$$CR = \frac{I_{corr} \times K \times EW}{\rho A} \quad (1)$$

Here the corrosion rate constant $K = 3272\ \text{mm year}^{-1}$, the equivalent weight $EW = 27.9\ \text{g}$, the material density $\rho = 7.85\ \text{g cm}^{-3}$ for MS, and the sample area $A = 14\ \text{cm}^2$.

The protection efficiency of EPD and EPB coatings was estimated with following equation:

$$E\ (\%) = \frac{I_{corr} - I_{corr(C)}}{I_{corr}} \times 100 \quad (2)$$

where I_{corr} and $I_{corr(C)}$ were the corrosion current values in the absence and presence of the coatings, respectively. The above corrosion parameters of all the samples are summarized in Table 1.

The Tafel curves for the EPB coated electrodes gave a E_{corr} higher than −500 mV, more positive than for bare MS at −704 mV and for the EPD samples at −525 mV. The positive shift in E_{corr} indicated that the protection of the MS surface by the EPB coatings was better than EPD coating. It was also observed that the EPB coated MS exhibited lower corrosion rate (<5.35×10^{-4} mm year^{-1}) compared to the bare MS (3.43×10^{-2} mm year^{-1}) and EPD samples. Finally, the protection efficiency of EPB samples was found to be more than 98%.

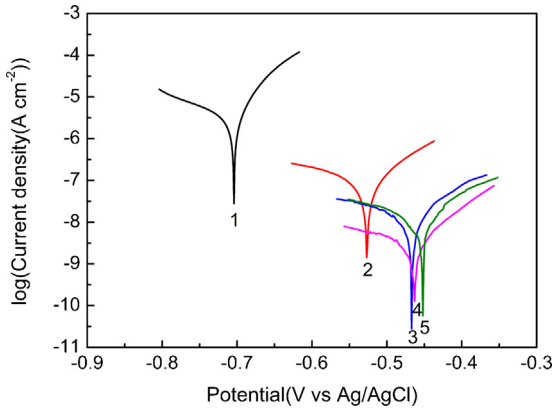

Fig. 5. Tafel curves for different electrodes measured in 3.5 wt% NaCl aqueous solution, 1: Bare MS; 2: EPD; 3: EPB20; 4: EPB30; and 5: EPB40.

Table 1
Results of electrochemical corrosion measurements for different samples in 3.5 wt% NaCl solutions.

Sample	Corrosion rate (mm year^{-1})	E (%)	R_{ct} (kΩ cm^2)
MS	3.43×10^{-2}	0	1.88
EPD	1.10×10^{-3}	96.79	4.36×10^{2}
EPB20	5.35×10^{-4}	98.44	1.11×10^{3}
EPB30	1.46×10^{-4}	99.51	1.87×10^{3}
EPB40	4.45×10^{-4}	98.50	1.56×10^{3}

EIS Bode plots (impedance vs frequency) of uncoated and coated MS are shown in Fig. 6. In this research, the fitting of all EIS data is performed using a simple equivalent electric circuit model (Fig. 6a), which is typically used for bare and coated MS [38]. This model includes the following elements: a resistor R_s related to resistance of the solution, a constant phase element (C_{dl}) to model the capacitance of the electrical double layer at the metal/liquid interface, and a resistor R_{ct} related to the polymer resistance, resistance at the metal–polymer interface or to the polymer–solution resistance [37,39,38]. It is suggested that a good superposition with the experimental data is observed by fitting EIS data with the model, and the uncertainty of R_{ct}s is less than 2%, which demonstrated the reliability of fitting results [40]. The resistance ability of the coating could be implied using R_{ct}, the higher the value the better the resistance [41]. Table 1 summarizes R_{ct} values obtained for the different samples. It was found that the highest charge transfer resistance of EPB, 1.87 MΩ cm^2 for EPB30, was four times larger than for EPD, and about three orders of magnitude larger compared with bare MS. The R_{ct} values of EPB20 and EPB40 were also much higher than EPD.

The protection performance of organic coatings is typically caused by the barrier ability against water and electrolytes [42,43]. The hydrophilic properties of epoxy inhibit its use as a coating material in humid conditions [2]. In this paper, it is shown that epoxy coatings with B-TMOS were much more hydrophobic than EPD samples. This increased hydrophobicity was beneficial to reduce the wettability of a corroding medium. In addition, the dual cross-linking and hydrogen-bonding network of polybenzoxazine and epoxy in EPB coatings would reduce porosity and enhance their barrier properties. EPB coatings presented superior corrosion resistance to bare MS and EPD coated MS electrodes, which were

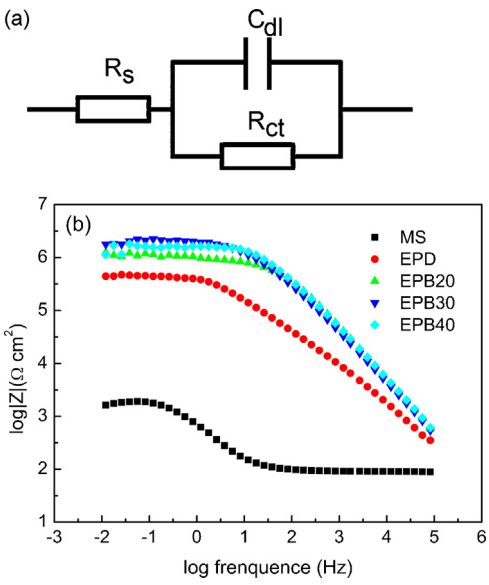

Fig. 6. (a) Analog circuit and (b) Bode graphs for different coated MS electrodes in 3.5 wt% NaCl aqueous solution.

verified by the consistent results among electrochemical measurements.

Meanwhile, it is also observed that the corrosion protection performance of EPB coated MS decreased after the initial increase with the increasing content of B-TMOS. Clearly, there are two stages where the corrosion resistance of EPB is changed. The first increase one, when B-TMOS content was low (<30 wt%), may be due to the increased curing degree of epoxy with the increasing content of curing agent (B-TMOS). Therefore, better film-forming property and higher corrosion protection ability is observed for completely cured EPB30 samples compare to ones with low (at 10 wt% or at 20 wt%) B-TMOS content.

The second stage, although epoxy is completely cured corresponding to B-TMOS content of 40 wt%, a drop in corrosion inhibition is observed. That is because some polybenzoxazine did not participate in the constitution of the hydrogen-bonding network, which is indicated by the existence of nonassociative free hydroxyl groups. It therefore may cause increase in the porosity of the coating. Hence, the corrosion resistance of EPB40 was lower than EPB 30. Therefore, 30 wt% is the optimal addition for B-TMOS as the curing agent for epoxy, which can balance the needs of curing epoxy and constructing the hydrogen-bonding network between polybenzoxazine and epoxy.

4. Conclusion

A silane-functional benzoxazine (B-TMOS) cured epoxy as a hydrophobic corrosion-inhibiting coating was successfully prepared on mild steel through a dip coating and thermal curing method. It was found that the surface hydrophobicity of B-TMOS cured epoxy coatings was enhanced significantly compared to DDM cured ones. The corrosion protection ability of epoxy coatings with 20–40 wt% B-TMOS content was also improved, which was investigated by following measurements with open-circuit potentials, potentiodynamic polarization curves and EIS methods. The results showed that the protection efficiency for bare MS of all EPB samples was more than 98% and the charge transfer resistance (R_{ct}) was approximately three orders of magnitude higher than for bare MS. Following a simple synthetic process, using non-fluorinated compounds, results in EPB coatings attractive for commercial application on the corrosion protection of MS.

Acknowledgments

This research was financially supported by the Nanotech Foundation of Science and Technology Commission of Shanghai Municipality (No. 0652nm001), the Fundamental Research Funds for the Central Universities, the National Natural Science Funds of China (Grant No. u1162110), Program of Shanghai Subject Chief Scientist (10XD1401500) and Lanpec Technologies Co., Ltd. The authors would like to thank to Dr. Ruben Mercade'-Prieto (Chemical Engineering, University of Birmingham) for his valuable helps with improving the language throughout the paper and polishing the English text.

References

[1] G. Schmitt, Global Needs for Knowledge Dissemination, Research, and Development in Materials Deterioration and Corrosion Control, World Corrosion Organization, New York, 2009.
[2] M.M. Popović, B.N. Grgur, V.B. Mišković-Stanković, Prog. Org. Coat. 52 (2005) 359–365.
[3] T.L. Metroke, J.S. Gandhi, A. Apblett, Prog. Org. Coat. 50 (2004) 231–246.
[4] C.-J. Weng, C.-H. Chang, C.-W. Peng, S.-W. Chen, J.-M. Yeh, C.-L. Hsu, Y. Wei, Chem. Mater. 23 (2011) 2075–2083.
[5] W.-G. Ji, J.-M. Hu, J.-Q. Zhang, C.-N. Cao, Corros. Sci. 48 (2006) 3731–3739.
[6] J.M. Hu, J.Q. Zhang, C.N. Cao, Prog. Org. Coat. 46 (2003) 273–279.
[7] X. Shi, T.A. Nguyen, Z. Suo, Y. Liu, R. Avci, Surf. Coat. Technol. 204 (2009) 237–245.
[8] S.-W. Kuo, W.-C. Liu, J. Appl. Polym. Sci. 117 (2010) 3121–3127.
[9] S.-Y. Zhang, Y.-F. Ding, S.-J. Li, X.-W. Luo, W.-F. Zhou, Corros. Sci. 44 (2002) 861–869.
[10] A.S. Castela, A.M. Simões, Corros. Sci. 45 (2003) 1631–1646.
[11] W.-G. Ji, J.-M. Hu, L. Liu, J.-Q. Zhang, C.-N. Cao, Prog. Org. Coat. 57 (2006) 439–443.
[12] N. Hameed, Q.P. Guo, T. Hanley, Y.W. Mai, J. Polym. Sci. Pt. B: Polym. Phys. 48 (2010) 790–800.
[13] M. Sangermano, F. Sordo, M. Messori, Macromol. Mater. Eng. 297 (2012) 257–262.
[14] X. Cui, Y. Gao, S. Zhong, Z. Zheng, Y. Cheng, H. Wang, J. Polym. Res. 19 (2012) 1–7.
[15] S. Rimdusit, P. Kunopast, I. Dueramae, Polym. Eng. Sci. 51 (2011) 1797–1807.
[16] S. Grishchuk, S. Schmitt, O.C. Vorster, J. Karger-Kocsis, J. Appl. Polym. Sci. 124 (2012) 2824–2837.
[17] H. Ishida, D.J. Allen, Polymer 37 (1996) 4487–4495.
[18] H. Kimura, A. Matsumoto, K. Hasegawa, K. Ohtsuka, A. Fukuda, J. Appl. Polym. Sci. 68 (1998) 1903–1910.
[19] H. Ishida, S. Ohba, T. J. Appl. Polym. Sci. 101 (2006) 1670–1677.
[20] H. Kimura, A. Matsumoto, K. Ohtsuka, J. Appl. Polym. Sci. 112 (2009) 1762–1770.
[21] L. Qu, Z. Xin, Langmuir 27 (2011) 8365–8370.
[22] H. Dong, Z. Xin, X. Lu, Y. Lv, Polymer 52 (2011) 1092–1101.
[23] J. Liu, X. Lu, Z. Xin, C. Zhou, Langmuir 29 (2013) 411–416.
[24] C.-F. Wang, S.-F. Chiou, F.-H. Ko, J.-K. Chen, C.-T. Chou, C.-F. Huang, S.-W. Kuo, F.-C. Chang, Langmuir 23 (2007) 5868–5871.
[25] Z. Xin, C. Zhang, X. Lu, CN 201210148147.6 (2012).
[26] D.E. Beving, A.M.P. McDonnell, W. Yang, Y. Yan, J. Electrochem. Soc. 153 (2006) B325.
[27] Y. Liu, W. Zhang, Y. Chen, S. Zheng, J. Appl. Polym. Sci. 99 (2006) 927–936.
[28] D. Zhu, W.J.V. Ooij, Electrochim. Acta 49 (2004) 1113–1125.
[29] J.-M. Yeh, C.-J. Weng, W.-J. Liao, Y.-W. Mau, Surf. Coat. Technol. 201 (2006) 1788–1795.
[30] L. Boinovich, A. Emelyanenko, Adv. Colloid Interface Sci. 179–182 (2012) 133–141.
[31] L.B. Boinovich, S.V. Gnedenkov, D.A. Alpysbaeva, V.S. Egorkin, A.M. Emelyanenko, S.L. Sinebryukhov, A.K. Zaretskaya, Corros. Sci. 55 (2012) 238–245.
[32] S.V. Gnedenkov, S.L. Sinebryukhov, D.V. Mashtalyar, V.M. Buznik, A.M. Emel'yanenko, L.B. Boinovich, Prot. Met. Phys. Chem. Surf. 47 (2011) 93–101.
[33] C. Zhou, X. Lu, Z. Xin, J. Liu, Corros. Sci. 70 (2013) 145–151.
[34] S. Radhakrishnan, C.R. Siju, D. Mahanta, S. Patil, G. Madras, Electrochim. Acta 54 (2009) 1249–1254.
[35] T. Tüken, A.T. Özyılmaz, B. Yazıcı, M. Erbil, Appl. Surf. Sci. 236 (2004) 292–305.
[36] B. Nikravesh, B. Ramezanzadeh, A.A. Sarabi, S.M. Kasiriha, Corros. Sci. 53 (2011) 1592–1603.
[37] D. Prasai, J.C. Tuberquia, R.R. Harl, G.K. Jennings, K.I. Bolotin, ACS Nano. 6 (2012) 1102–1108.
[38] T.-C. Huang, Y.-A. Su, T.-C. Yeh, H.-Y. Huang, C.-P. Wu, K.-Y. Huang, Y.-C. Chou, J.-M. Yeh, Y. Wei, Electrochim. Acta 56 (2011) 6142–6149.
[39] F. Chen, P. Liu, ACS Appl. Mater. Inter. 3 (2011) 2694–2702.
[40] S.-D. Xu, Q.-C. Zhuang, L.-L. Tian, Y.-P. Qin, L. Fang, S.-G. Sun, J. Phys. Chem. C 115 (2011) 9210–9219.
[41] E. Hür, G. Bereket, Y. Şahin, Prog. Org. Coat. 57 (2006) 149–158.
[42] J.-T. Zhang, J.-M. Hu, J.-Q. Zhang, C.-N. Cao, Prog. Org. Coat. 51 (2004) 145–151.
[43] D. Zhu, W.J. van Ooij, Corros. Sci. 45 (2003) 2177–2197.